

PAPER • OPEN ACCESS

6 DOF articulated-arm robot and mobile platform: Dynamic modelling as Multibody System and its validation via Experimental Modal Analysis.

To cite this article: A Toledo Fuentes *et al* 2017 *IOP Conf. Ser.: Mater. Sci. Eng.* **257** 012008

View the [article online](#) for updates and enhancements.

Related content

- [Density Matrix for Multibody System with Harmonic Coupling](#)
Bai ZhiMing, Wei JiangNan and Ge MoLin
- [Multibody systems dynamics for bio-inspired locomotion: from geometric structures to computational aspects](#)
Frédéric Boyer and Mathieu Porez
- [Urban search mobile platform modeling in hindered access conditions](#)
I I Barankova, U V Mikhailova, O B Kalugina *et al.*

Recent citations

- [A comparative study of PID and neuro-fuzzy based control schemes for a 6-DoF robotic arm](#)
Sachin Srivastava *et al*



IOP | ebooks™

Bringing you innovative digital publishing with leading voices
to create your essential collection of books in STEM research.

Start exploring the collection - download the first chapter of
every title for free.

6 DOF articulated-arm robot and mobile platform: Dynamic modelling as Multibody System and its validation via Experimental Modal Analysis.

A Toledo Fuentes^{1,*}, M Kipfmueller¹, M A José Prieto²

¹ Institute of Materials and Processes, University of Applied Science, Karlsruhe 76131, Germany

² Department of Electrical Engineering, University of Oviedo, Gijón 33203, Spain

*Corresponding author: aishe.toledo-fuentes@hs-karlsruhe.de

Abstract. Mobile manipulators are becoming a key instrument to increase the flexibility in industrial processes. Some of their requirements include handling of objects with different weights and sizes and their “fast” transportation, without jeopardizing production workers and machines. The compensation of forces affecting the system dynamic is therefore needed to avoid unwanted oscillations and tilting by sudden accelerations and decelerations. One general solution may be the implementation of external positioning elements to active stabilize the system. To accomplish the approach, the dynamic behavior of a robotic arm and a mobile platform was investigated to develop the stabilization mechanism using multibody simulations. The methodology used was divided into two phases for each subsystem: their natural frequencies and modal shapes were obtained using experimental modal analyses. Then, based on these experimental results, multibody simulation models (MBS) were set up and its dynamical parameters adjusted. Their modal shapes together with their obtained natural frequencies allowed a quantitative and qualitative analysis. In summary, the MBS models were successfully validated with the real subsystems, with a maximal percentage error of 15%. These models will serve as the basis for future steps in the design of the external actuators and its control strategy using a co-simulation tool.

1. Introduction

Recent developments in the field of the fourth industrial revolution have emphasized in the ambitious trends and achievement criteria in automate production [1, 2]. Most studies in this area have highly focused on the development of the so-called Internet of Things, underestimating all the technology that has to carry out the tasks in an autonomous way without critical limitations. In recent years, mobile manipulators based on costly light-weight robot arms mounted on the top of relatively bulky mobile autonomous platforms have been introduced in production lines to achieve a higher degree of flexibility in transport and handling tasks. However, this form of robotic solutions is limited by their restricted payload (nowadays, 14 kg maximal payload [3, 4]), avoiding the potential risk of losing their stability while the mobile platform moves through the plant. The demand for handling higher payloads implies the use of bigger manipulators (with higher center of gravity) mounted on large-footprint and heavier mobile platforms to prevent the robot arms from tipping over [5]. Likewise, large-footprint platforms are directly associated with more required workspace, and thus higher costs for the plant surface area. There is, therefore, a definite need to develop a robot system which comprises a high payload robot arm on a small-footprint autonomous mobile platform.



The first serious discussions and analyses aimed to stabilize mobile manipulators with a high center of gravity emerged in 1997 with Graf and Dillmann [6], implementing a parallel manipulator using a Stewart-platform to actively compensate any accelerations. Further examples of research include the optimization of this approach [7, 8, 9]. While it is an efficient way to ensure the stability during the transport of fragile objects on its platform base, the system is not designed to handle them. Besides that, some researchers (e.g. Zhao et al. [10]; Acar and Murakami [11]) have attempted to implement a three DOF manipulator on a two-wheeled mobile platform. They applied the inverted pendulum principle to model the robot system dynamic as one body: its center of gravity, an important parameter to keep the system stable, varies depending on displacements, velocities and accelerations of the mobile platform, as well as on the weight and height of the robot arm. The design approaches developed at the Institute for Cognitive Systems at the Technical University of Munich [12] as well as at the Korea Institute of Science and Technology [13] and at the Fraunhofer Institute of Optronics in Karlsruhe [14] consist of a two-arm humanoid upper body. The robot body is mounted on a “Compact Omni-directional Mobile Platform” and on Segway devices, respectively, to allow it to be moved.

Such approaches, however, have tended to focus on the development of completely new robotic systems rather than the design of an active external mechanism to ensure the system stability at standstill or during normal plant operation, regardless of the robot arm and mobile platform model. In order to realize this concept, an upgradeable system is proposed: With in the fabric currently available robot arms and an active external actuator system, an affordable mobile manipulator could be built, simply by integrating them with a small footprint platform. The particular importance of this approach lies in the possible use of low-cost robot arms or the re-use of already existents in the plant.

The main challenge to face in the design of the actuator system is to guarantee the stability of the manipulator during its operation, including when the mobile platform abruptly starts or stops. In other words, the system should react to any external influences and, consequently not to affect the human safety in the working areas [15]. Their adequate control strategy to compensate the accelerations should ensure the equilibrium of dynamical forces affecting the system balance in every moment.

As an essential phase of the development process, the performance of the control strategies to be implemented should be evaluate under critical conditions using multibody simulation models. These developed dynamical models should resemble as accurate as possible the real testing system [16], consisting of a mobile robotic platform (see figure 1) and an articulated-arm robot (see figure 2).

This paper focused on the modelling process of both mentioned robots as multibody systems by adapting the procedure used in [17]: As a first step, the dynamic properties (modal shapes and natural frequencies) of each real robot were separately identified by means of experimental modal analyses. Subsequently, CAD-Models of each robotic system were prepared in order to build them as multibody models into a MBS-Software (MSC.Adams/View). The obtained experimental findings (from experimental modal analyses) were compared with the results produced by the multibody simulation. By adjusting the modal parameters of the simulative models, the dynamic behaviors of the real system were replicated. Thus, the expected result will be the development of close to reality MBS models of the testing systems. Further information about this method is presented in [18, 19].



Figure 1. Robot I to be modelled: Autonomous mobile platform (MetraLabs X3).



Figure 2. Robot II to be modelled: 6 DOF articulated-arm robot (Mitsubishi RV-3AL).

2. Experiment / Simulation set up

2.1. Identification of modal parameters via experimental modal analysis

The dynamic behavior of any system can be estimated by means of modal analysis. The so-called experimental modal analysis consists in exciting externally a real mechanical system (input forces) and in measuring its dynamic behavior in response to the applied stimulus (output accelerations). This Response Function describes the relation force/acceleration and allows to validate simulation models of multibody systems.

The presented study seeks to obtain experimental data which will help to validate the dynamical models of robotic systems.

The correct election of the excitation and measurement form were the initial aspects to consider in order to perform a proper experimental modal analysis (the abbreviation EMA will be used hereafter to refer to it). For this particular set up, the relevant parameters for the impulse hammer (including tip), 3D accelerometers and the measurement frequency range are shown in table 1.

Table 1. Configuration parameters for the experimental modal analyses.

Parameter	Value (for both robotic systems)
Measured Response Frequency range	800 Hz
Impulse hammer – Tip	Soft impact tip
Impulse hammer – Weight / sensitivity	1.0 pound / 1.0 mV/LB
Accelerometer – Voltage Sensitivity	1.0 +12/-8% mV/ms ⁻²
	10 ±10% mV/g

The election of the suitable excitation and measurement points was another important object of analysis. The challenge lay in choosing the proper points without having previous knowledge about the dynamic behavior of the real systems. In our case, the risk of ignoring some natural frequencies and modal shapes during the excitation or measuring was low, as long as the excitation points were consciously collocated non orthogonal to the measurement points (all orthogonal shapes concerned to the impact force direction may not be measured by the accelerometers [20]). The excitation and measuring conditions, the used impulse hammer, tip and hammer head as well as the sensors, excitation/measurement points and their directions were the same for all tests.

Although the analysis was carried out in a frequency range from 0 Hz to 800 Hz, the most important frequencies were expected within a low frequency range, under 100 Hz.

2.1.1. EMA of mobile platform. First, the structure of the mobile platform was analyzed. The red plastic covering (see figure 1) was removed in order to identify all the surfaces where the sensors had to be placed and the force impacts had to be applied. The 3 excitation points (see green dots in figure 3) were selected to guarantee the application of stimulus in all coordinates of the Cartesian space. Each experimental series consisted in an excitation of 5 stimuli with delays between each other using the same impulse hammer. Additionally, the 25 chosen measuring points were mainly collocated on the rigid aluminum profiles and near to the screw joints to ensure a good reproduction of the system oscillation but do not emulate the vibration of each single element. These points were the basis for the geometry built into the processing software OROS Modal 2 (see figure 4), which would graphically display the platform modal shapes as result of the EMAs.

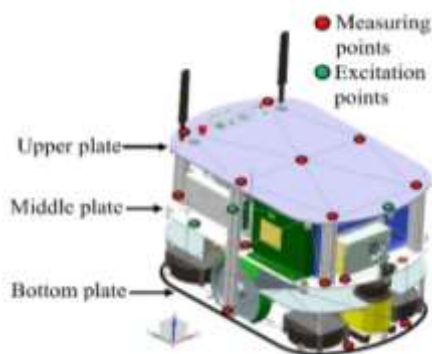


Figure 3. CAD model of the mobile platform and its measurement points.

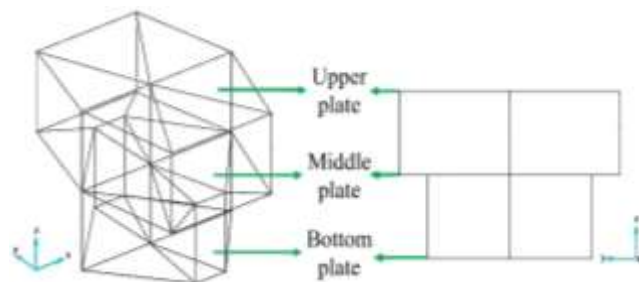


Figure 4. Representation of the mobile platform in OROS Modal 2 (based on the points in figure 3).

2.1.2. EMA of articulated-arm robot. The EMA of the articulated-arm robot was carried out in Home configuration, as presented in the figure 5.

Similar to the mobile platform, the system was analyzed, and the excitation and measurement points that guaranteed an appropriate excitation and detection of the whole modal parameters were identified (see red dots in figure 5): The simplification of the robot geometry in OROS Modal 2, shown in figure 6, resulted in 8 excitation points and 23 measurement points.

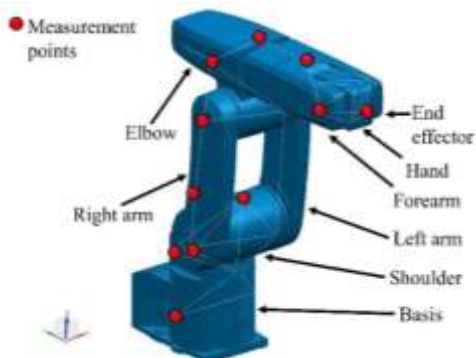


Figure 5. CAD model of the articulated-arm robot and its measurement points.

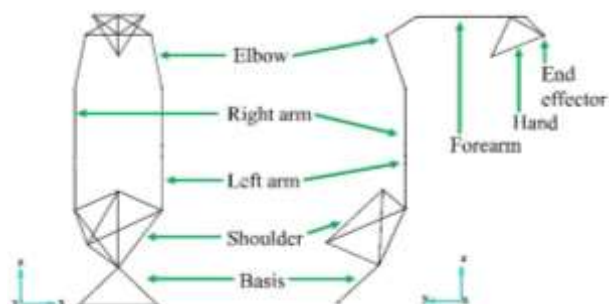


Figure 6. Representation of the main parts of the articulated-arm robot in OROS Modal 2.

2.2. Modelling of multibody systems

The attainment of the experimental analyses, in terms of natural frequencies and modal shapes, allowed the reliable modelling of the mobile platform and the articulated-arm robot as multibody systems. The modelling process started with the analysis of the system dynamic behavior according to the information obtained from the EMAs. Hence, the systems were modelled with a low level of detail to get good computing performance, but as complex as the reproduction of the real dynamic behavior may not be affected by excluding some elements in the model (see “Model validation”). In other words, the multibody systems had to contain justly all necessary information to describe the dynamic phenomenon of the real mobile platform and articulated-arm robot.

During this analysis, the potential to model the structure of both systems as rigid bodies in the MBS was detected: No relevant deformations appears in the main bodies of the structures in comparison to the elastic joint elements, which were responsible to generate the detected model shapes (see 4.1- 4.2).

2.2.1. MBS of mobile platform. In order to build the MBS model of the mobile platform, the estimation of the inertial parameters was carried out based on its CAD model, which contained all the information about its geometry and materials. This CAD model with inertial properties was exported into the used multibody simulation software, MSC.Adams/View.

According to [21] there are different variants to model bodies as MBS systems: rigid, elastic and their combination (so-called hybrid). In the cases presented in this paper, all bodies were implemented as rigid (except for the joints elements), since the purpose was not to represent the deformation of each particular element of the system when a force is acting on them, but rather to reproduce the oscillation of the whole system into a fixed space. This implied that each element tends to suffer an insignificant deformation in comparison to the oscillation of the whole system exhibited from EMA.

In order to simplify the system, elements with the same material were merged into one. Without considering the red outer covering, each element of the structure was examined to determine its possible influence in the oscillation phenomenon: screws, screw nuts, washers and slot nuts were removed and replaced by fix joints.

The next step was to connect each of the rigid bodies using massless elastic joint elements. They defined the degree of freedom of the whole mobile platform, and thus, restrict the number of the modal shapes within the low frequency range. All existing joint elements of the real mobile platform were classified based on their kinematic (geometrical relation) and their physical force properties, acting between two or more links [22]. The most influential components were recognized between the drive wheel and the aluminum support: wheel suspensions, swing arms, dampers, spacer sleeves and rigid struts. To define the systems degrees of freedom and thus to limit the constraining forces affecting their bodies, so-called kinetic virtually joints with floating characteristics had to be implemented in the model. These massless elastic joint elements are shown in table 2. The drive wheels were fixed to the ground.

Table 2. Joint elements implemented between the main rigid bodies of the mobile platform.

Joint elements found in the real mobile platform	Massless joint elements used in the MBS
Cylinder-piston system / spacer sleeves	Damper and linear spring / Bushing
Drive shaft and bearings	Bushing
Coupling and motor shaft	Torsion spring
Rigid strut and structure	Bushing
Swing arm and structure	Linear and torsion spring

The modelling of those elements, together with their inherent stiffness and damping parameters, enabled the dynamic oscillation of the system. A first estimation of these parameters for each joint element was performed via Finite Element Analysis. The multibody model was dynamically simulated with these first approximations: The results obtained in terms of natural frequencies and their corresponding modal shapes were analyzed and compared with the experimental findings from the EMA. If there was no coincidence between the experimental and the simulative procedure, the stiffness and damping coefficients of specific joints had to be adjusted until the results were equivalent. The visualization of the modal shapes in the simulations presented a helpful qualitative analysis to identify which specific joint element had to be modified and how much.

2.2.2. MBS of articulated-arm robot. The modelling of the articulated-arm robot in MSC.Adams/View was very similar to the procedure followed for the mobile platform, but with a main difference: It available CAD model just contained information merely related to sizes and geometries, but not aspects about materials, weight, center of mass and moment of inertia, which played a crucial role in the modelling process. The bodies with bigger and heavier properties may mainly affect the dynamic behavior of the system because of their inertial properties. A material identification was carried out, in particular, to estimate the density of the materials in the outer structure by performing some simple non-destructive tests (Archimedean principle as well as magnetic proof). Then, the material specifications were introduced into the shell CAD model and were adjusted so as to match up the weight specified by the robot manufacturer. This detailed model with centers of mass and moments of inertia was exported into MSC.Adams/View.

The model simplification of the robot was achieved by identifying all the mechanical joints existing in the real robot (based on [23]). Analogous to the mobile platform, the robot components with the

higher mass and inertial moment were abstracted and merged into basic elements: Basis, shoulder, right arm, left arm, elbow, forearm, hand and end effector (see figure 6). They were modelled as rigid bodies for the same reason as the mobile platform.






These 8 basic elements were joined to each other using the so-called bushings, massless elastic joint elements with up to 6 DOF, which can replicate both translational and rotational constraints by introducing certain stiffness and damping values for each available degree of freedom; in every joint, they reproduced kinematic effects and, during a dynamic simulation, applied forces and torques to each junction point. For the articulated-arm robot, each bushing had to allow only one rotational DOF, emulating the motors in the robot joints. The correlation between the rigid bodies and the entire set of bushings in the system defined the robot oscillation behavior. Detailed information about MBS methodologies could be found in [23, 24].

3. Model validation

3.1. EMA and MBS: Mobile platform

The results of the EMA for the mobile platform are shown in the table 3. An overlapping method [25] allowed to identify the first eight natural frequencies (ω) under 100 Hz: The first, third and fourth natural frequencies (7 Hz, 21 Hz and 28 Hz) appeared in all tests. Following the overlapping method, the remaining values were obtained at 10 Hz, 54 Hz, 62 Hz, 75 Hz and 81 Hz, which were visible just in no more than two different directions of excitation. The corresponding first five modal shapes are graphically represented in the table 3.

Table 3. Modal shapes and natural frequencies of the mobile platform obtained from the EMAs.

Natural freq. and modal shapes	$\omega_1 = 7.75$ Hz	$\omega_2 = 10.3$ Hz	$\omega_3 = 21.4$ Hz	$\omega_4 = 28.0$ Hz	$\omega_5 = 54.0$ Hz
EMA Mobile platform					




The grey lines in the modal forms represent the initial state, the red lines the maximum amplitude attained, the yellow lines the proportionately smaller amplitudes and the blue lines the smallest one. Taking figure 4 as reference for the geometry, the first modal shape from table 3 consisted in a rotation of the platform about the Z-axis (yaw). The second modal shape showed a translational movement in X-direction. The third one exhibited a petty rotation around the Y-axis (roll) and another around the X-axis (pitch). The fourth and fifth modal shapes displayed a slightly tilting around the Y-axis (roll) and the X-axis (pitch), respectively. All axes are related to the light blue coordinate system.

After completing the multibody modelling of both systems with rigid bodies and massless joint elements, proceed the validation of these simulation models: Their stiffness and damping parameters had to be iteratively adjusted as long as the simulation reproduced similar natural frequencies and modal forms related to the experimental results.

For both mobile platform and articulated-arm robot the modal shapes from EMA were the key to validate the calculated natural frequencies of the MBS: The modal shape of the desired natural frequency had to exhibit the same oscillation as in the real system (from EMA). Thus, the natural frequency could be validated and the iterative process was concluded.

The results for the mobile platform after the adjustment of their natural frequencies and modal shapes are shown in the table 4. The red traces in the illustrations represent the modal shapes.




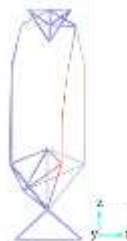

Table 4. Modal parameters of the mobile platform obtained from multibody simulations.

Natural freq. and modal shapes	$\omega_1= 8.92$ Hz	$\omega_2= 12.96$ Hz	$\omega_3= 21.54$ Hz
MBS Mobile platform			

3.2. EMA and MBS: 6DOF articulated-arm robot

Analogous to the mobile platform, the table 5 gives the first natural frequencies and modal shapes from EMA acquired by the excitation of the system in different directions.

Table 5. Modal shapes and natural frequencies of the articulated-arm robot obtained from the EMAs.






Natural frequencies and modal shapes	$\omega_1= 11.0$ Hz	$\omega_2= 21.0$ Hz	$\omega_3= 27.0$ Hz	$\omega_4= 72$ Hz	$\omega_5= 89$ Hz
EMA Articulated-arm robot					

It was observed that the first three natural frequencies (11 Hz, 21 Hz and 27 Hz) were found in all directions of excitation. However, the natural frequencies at 72 Hz and 89 Hz appeared only in two separately excitation points. All frequencies of interest were found within the first 100 Hz.

Each modal shape, and thereby the natural frequencies, depended on the current position of the system. For the illustrated home position, the first modal shape (at 11 Hz) was a pitching movement (around the X-axis) generated by the elbow, the forearm and the end effector; the second and third modal shapes (21 Hz and 27 Hz) affected only the lightest four components, causing a slightly rolling movement around the Z-axis and a rotation around the X-axis (pitching) in the elbow, forearm, hand and end effector; the fourth modal shape (at 89 Hz) presented a deflection on the left arm; and finally, the fifth modal shape also showed a slightly pitching movement (rotation around X-axis) but just starting in the hand and continuing with the end effector.

Likewise, in the same way as for the mobile platform, these experimental outcomes were the reference for the successive adjustment of the stiffness and damping parameters in the multibody simulation model. These simulation results are presented in table 6. The red traces in the illustrations represent the modal shapes.

Table 6. Modal parameters of the articulated-arm robot obtained from the multibody simulations.

Natural frequencies and modal shapes	$\omega_1= 13.0$ Hz	$\omega_2= 22.5$ Hz	$\omega_3= 27.2$ Hz	$\omega_4= 68.3$ Hz	$\omega_5= 88.9$ Hz
MBS Articulated-arm robot					

4. Results and discussion

The graphic in figure 7 presents the calculation of the MBS reliability related to the EMA, using the “three-sigma limit” method [26]. The natural frequencies from EMA are represented by the black solid line. It can be seen that the first modal frequency of the MBS (red solid line) was not kept within the calculated limits (grey and green dashed lines) in contrast to the second and third values, which are in the tolerated area. The deviation of this first natural frequency is about 15%, which could have been caused by the model simplification procedure. Despite this and according to [27, 28], this value could be considered as a good approximation.

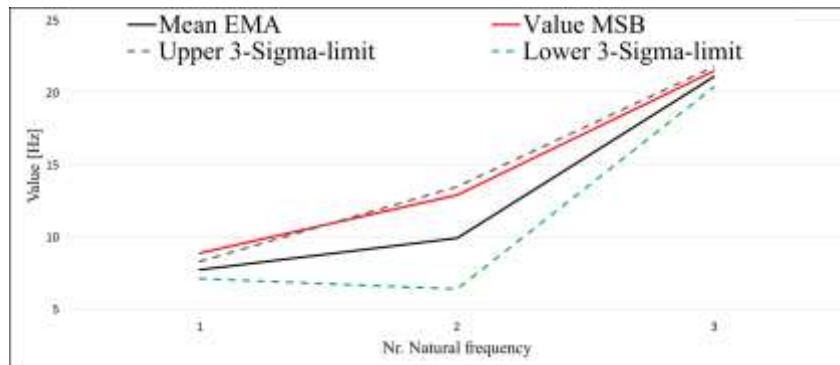


Figure 7. Correlation between EMA- and MSB-mobile platform using 3-sigma limits.

Meanwhile, the MBS of the articulated-arm robot presented a better fitting (see figure 8). However, the second natural frequency was slightly outside of the tolerance margin either (red solid line). Although this deviation between the MBS and the EMA (black solid line) resulted about 10.6%, it fulfilled the condition mentioned above [27, 28]. As can be seen from the graphic, the remaining values were within the “three-sigma limits”.

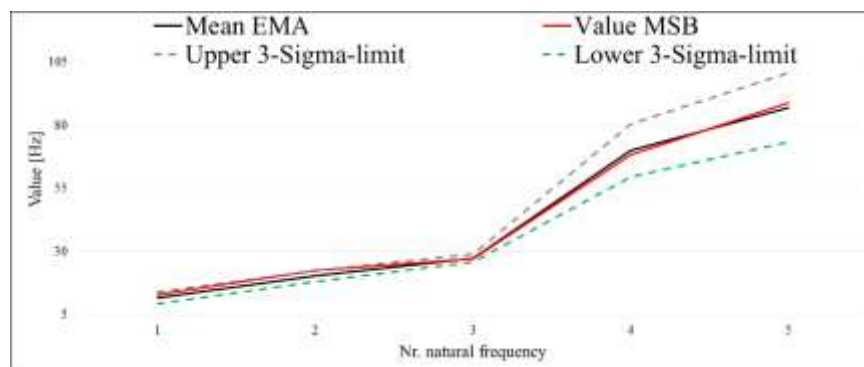


Figure 8. Correlation between EMA- and MSB-articulated arm robot using 3-sigma limits.

Hence, some variations between the MBS- and the EMA- results could have been caused, on the one hand, by the model simplification carried out to decrease the complexity of the systems (e.g. friction coefficients of the components were not experimentally determined, rigid bodies were used to avoid large computational calculations, etc.). On the other hand, random errors could have emerged due to parametric uncertainties as lack of material homogeneity, tolerances in the geometry, unknown clearance between the robot elements, etc., having non-ideal real conditions as in MBS models.

5. Mechatronic simulation

Once both systems were modelled and validated, it was possible to join them into a whole mobile manipulator model. This new MBS system had to be integrated with external actuators, whose task should be the dynamic compensation of external forces to assure its equilibrium, and thus to prevent the manipulator from tilting by abrupt acceleration and deceleration events. The whole system is shown in figure 9. In order to speed up the design and testing phase of the required control strategy for

the integrated actuators, a co-simulation between MatLab/Simulink and MSC.Adams/View must be performed: the closed loop control of the external actuators communicates with the dynamic MBS and sends the control signals to each of them; the MBS, as feedback loop, returns measurements from virtual sensors as force, angle, speed, acceleration, etc., at certain time intervals. The figure 10 illustrates the coupled simulation. Currently, the integrated model is used to develop control algorithms for the system's active stabilization. A full discussion about the selection process, the design and testing phase of the actuators lies beyond the scope of this article.

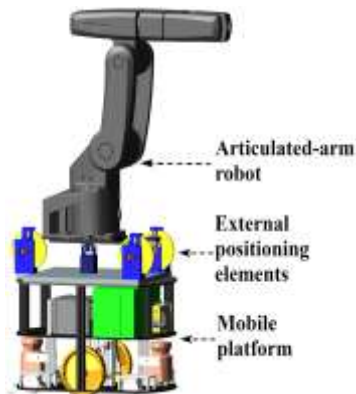


Figure 9. MBS-mobile manipulator.

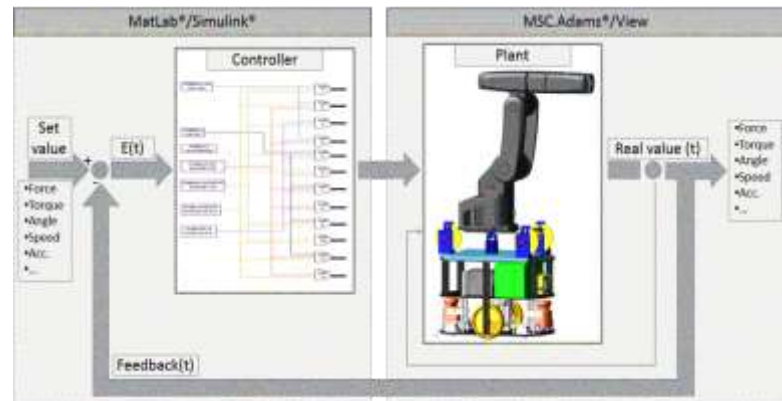


Figure 10. Schema of the co-simulation loop.

6. Conclusions

The aim of the present article was to determine experimentally the dynamic behavior of two robotic systems and, based on the results achieved, to model them as multibody simulations. At the first stage, experimental modal analyses have identified the natural frequencies and modal shapes of both real systems. These experimental results supported the implementation of rigid bodies in the multibody simulation to model all the components of both systems (except for their elastic joint elements). A key strength of their modelling as MBS was to define the stiffness and damping values for all joint elements of the systems. Each dynamical simulation generated magnitudes of natural frequencies depending on those stiffness and damping values. Together with their corresponding modal shapes, they were compared with the empirical values until they matched suitably to perform the development of the control strategy for the active stabilization.

The findings verified the good reproduction of the dynamical behavior of the real systems in the multibody simulation models. Although the current study is based on particular robots, it offers a helpful insight into the methodology for further complex systems, especially with regards to mobile platforms, whose dynamic behavior still little known.

A limitation of the implemented MBS modeling technique, particularly for the mobile platform, was the iterative adjustment process of the stiffness and damping values to obtain the desired natural frequencies. This suggested moving on to discuss the demand to improve this method. What is now needed is the development of an automated optimization algorithm able to mathematically determine the approximate stiffness and damping values for each joint element of the system. All these resulting parameters together would be reflected in their proper natural frequencies and modal shapes (see 3.2.), thereby avoiding the time-consuming manual iterative process. Thus, the articulated-arm robot could be easily modeled in different poses (e.g. in vertical and horizontal configuration) for further investigations. The authors are currently working on the implementation of those optimization strategies in a second investigation project.

The described MBS model is currently used to complete the development of the control strategy based on mechatronic co-simulations. The control system should ensure the stability of the whole mobile manipulator under accelerations and decelerations. Alongside, the optimization of its functionality should be carried out, taking in account sensitivity studies for the simulation model. The intention is to implement the control algorithm in a prototype developed and already set up by the authors without making relevant changes.

Acknowledgement

The authors would like to thank the state Baden-Württemberg for the kind support within the funding program “Innovative Projekte”.

References

- [1] Qin J, Liu Y and Grosvenor R 2016 A categorical framework of manufacturing for industry 4.0 and beyond *Procedia 6th CIRP Int. Conf. CARV (September 4-6, Bath)* vol 52 ed A Nassehi and S Newman (Amsterdam: Elsevier) pp 173-8
- [2] Schleipen M, Gilani S S, Bischoff T and Pfrommer J 2016 Industrie 4.0 - enabling technology with high diversity and variability *Proc. 49th CIRP Conf. Manufacturing Systems (May 25-27, Stuttgart)* vol 57 ed E Westkämper and T Bauernhansl (Amsterdam: Elsevier) pp 315-20
- [3] Fang H, Lijie G and Shaoping B 2015 A light weight arm designed with modular joints *Proc. 3rd IFToMM Symp. on Mechanism Design for Robotics (Mechanisms and machine science vol 33) (June 2-4, Aalborg)* ed B Shaoping and M Ceccarelli (Switzerland: Springer) p 49
- [4] SCHUNK Mobile Greifsysteme 2017 Powerball Lightweight Arm / Dextrous Lightweight Arm Available from: <http://www.schunk-mechatronik.com/startseite/schunk-mobile-greifsysteme.html> [Accessed 26th July 2017]
- [5] Acar C and Murakami T 2008 Underactuated two-wheeled mobile manipulator control using nonlinear backstepping method *Proc. 34th Annual Conf. IEEE IECON (November 10-13, Orlando)* (Piscataway, NJ: IEEE) pp 1680-5
- [6] Graf R and Dillmann R 1997 Active acceleration compensation using a Stewart-platform on a mobile robot *Proc. 2nd EUROMICRO Workshop on Advanced Mobile Robots (October 22-24, Brescia)* (Los Alamitos, California; Piscataway, NJ: IEEE) pp 59-64
- [7] Dang A X H and Ebert-Uphoff I 2004 Active acceleration compensation for transport vehicles carrying delicate objects *IEEE Trans. Robot.* **20** 830-9
- [8] Bai X, Davis J, Doebbler J, Turner J D and Junkins L J 2007 Dynamics, control and simulation of a mobile robotic system for 6-DOF motion emulation *Proc. WCECS (October 24-26, San Francisco)* ed S I Ao et al (Newswood Limited) pp 753-8
- [9] Danko T W, Chaney K P and Oh P Y 2015 A parallel manipulator for mobile manipulating UAVs *Proc. 7th IEEE Int. Conf. TePRA (May 11-12, Woburn)* (Piscataway, NJ: IEEE) pp 1-6
- [10] Zhao Y, Woo C and Lee J 2015 Balancing control of mobile manipulator with sliding mode controller *Proc. 15th ICCAS (October 13-16, Busan)* (S.I.: IEEE) pp 802-5
- [11] Acar C and Murakami T 2011 Multi-task control for dynamically balanced two-wheeled mobile manipulator through task-priority *Proc. 20th IEEE ISIE (June 27-30, Gdansk)* (Piscataway, NJ: IEEE) pp 2195-200
- [12] Leboutet Q, Dean-León E and Cheng G 2016 Tactile-based compliance with hierarchical force propagation for omnidirectional mobile manipulators *Proc. 16th IEEE RAS Int. Conf. Humanoid Robots (November 15-17, Cancun)* ed T Asfour (Piscataway, NJ: IEEE) pp 926-31
- [13] Cha Y S, Kim K G, Lee J Y, Lee J, Choi M, Jeong M H, Kim C H, You B J and Oh S R 2011 MAHRU-M: A mobile humanoid robot platform based on a dual-network control system and coordinated task execution *Rob. Auton. Syst.* **59** 354-66
- [14] Milighetti G, Petereit J and Kuntze H B 2010 Mobile experimental platform for the development of environmentally interactive control algorithms towards the implementation on a walking humanoid robot *Proc. 41st ISR and 6th ROBOTIK (June 7-9, Munich)* (S.I.: VDE) pp 682-8
- [15] Brettel M, Fischer F G, Bendig D, Weber A R and Wolff B 2016 Enablers for self-optimizing production systems in the context of industrie 4.0 *Proc. 48th CIRP Conf. Manufacturing Systems (June 24-26, Ischia)* vol 41 ed R Teti (Amsterdam: Elsevier) pp 93-8
- [16] Karnopp D C, Margolis D L and Rosenberg R C 2012 *System dynamics: Modeling, simulation, and control of mechatronic systems* (New Jersey: John Wiley & Sons) p 4

- [17] Webhofer M 2000 *Modellierung eines Mehrkörpersystems zur Simulation der Querschwingbewegung von Einseilumlaufbahnen bei der Stationseinfahrt* (Student research project TU Munich, Institute of Materials Handling, Material Flow, Logistics)
- [18] Rahnejat H and Rothberg S 2004 *Multi-body dynamics: Monitoring and simulation techniques III* (London and Bury St Edmunds: John Wiley & Sons) pp 373-90
- [19] Bauchau O A 2010 *Flexible multibody dynamics* (Dordrecht – Heidelberg – London - New York: Springer) pp 571-77
- [20] Karim A, Verl A and Höhne R 2014 Schwingungsanalyse an Bearbeitungsrobotern: Durchführung einer experimentellen Modalanalyse an Industrierobotern *wt online* **1/2-2014** 49
- [21] Kreuzer E, Lugtenburg J B, Meißner H G and Truckenbrodt A 2012 *Industrieroboter: Technik, Berechnung und anwendungsorientierte Auslegung* (Berlin - Heidelberg: Springer)
- [22] Gross D, Hauger W, Schröder J, Wall W and Govindjee 2014 *Engineering mechanics 3: Dynamics* (Berlin - Heidelberg: Springer)
- [23] Blundell M and Harty D 2014 *The multibody systems approach to vehicle dynamics* (Oxford - Massachusetts: Butterworth-Heinemann)
- [24] Bremer H 2008 *Elastic multibody dynamics: A direct Ritz approach* (Netherlands: Springer)
- [25] Neugebauer R, Kolouch M, Richter M and Schulten M 2009 Fehlerquellen bei einer Modalanalyse: Untersuchung von Einflussfaktoren während der praktischen Durchführung *wt online* **11/12-2009** 889-94
- [26] Devore J L, Farnum N R and Doi J A 2013 *Applied statistics for engineers and scientists* (Stamford: Cengage Learning) p 257
- [27] Kipfmüller M and Munzinger C 2009 Efficient simulation of parallel kinematic machine tools *Proc. ASME IDETC/CIE 33rd Mechanisms and Robotics Conf. (August 30- September 2, San Diego)* vol 7 (ASME) pp 523-30
- [28] Vinayak H and Singh R 1998 Multi-body dynamics and modal analysis of compliant gear bodies *J. Sound Vib.* **210** 171-214